Nuclear Engineering and Design 275 (2014) 229–241

Contents lists available at ScienceDirect

Nuclear Engineering and Design

journal homepage: www.elsevier.com/locate/nucengdes

The importance of input interactions in the uncertainty and sensitivity analysis of nuclear fuel behavior

T. Ikonen*, V. Tulkki

VTT Technical Research Centre of Finland, P.O. Box 1000, FI-02044 VTT, Finland

HIGHLIGHTS

- Uncertainty and sensitivity analysis of modeled nuclear fuel behavior is performed.
- Burnup dependency of the uncertainties and sensitivities is characterized.
- Input interactions significantly increase output uncertainties for irradiated fuel.
- Identification of uncertainty sources is greatly improved with higher order methods.
- Results stress the importance of using methods that take interactions into account.

ARTICLE INFO

Article history:
Received 13 June 2013
Received in revised form 5 May 2014
Accepted 16 May 2014

ABSTRACT

The propagation of uncertainties in a PWR fuel rod under steady-state irradiation is analyzed by computational means. A hypothetical steady-state scenario of the Three Mile Island 1 reactor fuel rod is modeled with the fuel performance FRAPCON, using realistic input uncertainties for the fabrication and model parameters, boundary conditions and material properties. The uncertainty and sensitivity analysis is performed by extensive Monte Carlo sampling of the inputs' probability distribution and by applying correlation coefficient and Sobol' variance decomposition analyses. The latter includes evaluation of the second order and total effect sensitivity indices, allowing the study of interactions between input variables. The results show that the interactions play a large role in the propagation of uncertainties, and first order methods such as the correlation coefficient analyses are in general insufficient for sensitivity analysis of the fuel rod. Significant improvement over the first order methods can be achieved by using higher order methods. The results also show that both the magnitude of the uncertainties and their propagation depends not only on the output in question, but also on burnup. The latter is due to onset of new phenomena (such as the fission gas release) and the gradual closure of the pellet-cladding gap with increasing burnup. Increasing burnup also affects the importance of input interactions. Interaction effects are typically highest in the moderate burnup (of the order of 10–40 MWd/kgU) regime, which covers a large portion of the operating regime of typical nuclear power plants. The results highlight the importance of using appropriate methods that can account for input interactions in the sensitivity analysis of the fuel rod behavior.

1. Introduction

The nuclear fuel rod of a light-water reactor consists of an oxide fuel pellet stack enclosed inside a metallic cladding tube. The pellet stack is held in place by a spring and the rod is pressurized with heat-conducting gas, facilitating heat transfer across the gap between the pellets and the cladding. Analysis of the fuel rod's behavior under irradiation in a nuclear reactor involves solving the transfer of heat from the pellet into the surrounding coolant through the gap and the cladding, the mechanical response of the pellet and the cladding to thermal and mechanical stresses, the irradiation-induced changes in materials, and the release of gaseous fission products into the gas gap. All the phenomena are interconnected, constituting an extremely complex system with rich behavior in different operating regimes and strong dependency on burnup (Bailly et al., 1999; Cacuci, 2010).

The system can be modeled numerically with dedicated fuel performance codes, which traditionally focus either on the steady

* Corresponding author. Tel.: +358 40 659 2130; fax: +358 20 722 5000.
E-mail address: timo.ikonen@vtt.fi (T. Ikonen).

http://dx.doi.org/10.1016/j.nucengdes.2014.05.015
0029-5493/

state irradiation or the simulation of transient scenarios. In both cases, one of the main purposes of numerical modeling is to provide understanding on how the individual phenomena interact and create the overall response of the rod to external conditions. An important aspect of such a study is the acquisition of detailed data that can be used to ensure that the rod performs within the safety and regulatory guidelines, and also to guide in revising the safety regulations (Rashid et al., 2011).

There are several sources of uncertainty in fuel performance analysis. The rod's fabrication parameters, experimentally determined material properties and system parameters are never precise, but introduce various amounts of uncertainties into the system. These are propagated to model outputs such as the fuel centerline temperature, internal pressure and gap conductance. To ensure safe operation of the fuel rod, these uncertainties must be taken into account, either by conservative analysis or best estimate analysis accompanied by evaluation of the related uncertainties. In best estimate analysis quantifying both the magnitude and the source of the output uncertainties is necessary. The latter involves determining the contribution of the uncertainty of each model input to the overall output uncertainty, and is called sensitivity analysis.

Sensitivity analysis in nuclear engineering has recently concentrated mostly on the reactor physics and neutronics and, on the other hand, on thermal hydraulic modeling. Sensitivity analysis of the fuel behavior models has received considerably less attention, although it is known that uncertainties related to fuel modeling can be significant and may also have broader impact on the thermal hydraulics and neutronics modeling (Christensen et al., 1981; Wilderman and Was, 1984; Syrjälahti, 2006; Boulore et al., 2012). In addition, most studies focus on the direct (first-order) effects of the input on the model output. A common approach is to evaluate, *e.g.*, the Spearman correlation coefficients or the first-order Sobol' indices from the model output (Boulore et al., 2012; Glaeser, 2008), which neglect the higher order interactions between the input variables. However, for a complex system such as the fuel rod (Rashid et al., 2011), these interactions can play a major role in the overall output uncertainties, and should not be neglected *a priori* (Saltelli et al., 2008).

In this paper, we investigate the role of input interactions in the uncertainty and sensitivity analysis of the nuclear fuel rod. For this purpose, we use the FRAPCON fuel performance code (Geelhood et al., 2011a,b) and perform statistical analysis of the code's output by evaluating both the conventionally used Spearman correlation coefficients (Draper and Smith, 1998; Kvam and Vidakovic, 2007) and the Sobol' sensitivity indices (Saltelli et al., 2008; Sobol', 1993). We consider a steady state scenario, and focus on identifying the major sources of uncertainties, characterizing interactions between inputs and their dependencies on burnup. Since the initial states of transient calculations with non-fresh fuel are usually generated by such steady state simulations, our results have direct relevance for transient analyses also.

The structure of the paper is as follows. In Section 2, we discuss the fuel performance code FRAPCON-3.4 used in the analysis of the scenario, and in Section 3 we describe the statistical analysis methods. The specifications of the modeled scenario and the input uncertainties are given in Section 4. In Section 5, we first show the best estimate plus uncertainty results of the scenario. Then, we illustrate how the data can be analyzed with the conventional methods and show that such an analysis remains incomplete in most cases. In Section 5.4, we repeat the analysis using the Sobol' variance decomposition method. We show that the variance decomposition analysis gives a consistent and much more complete picture of the system's response to the input uncertainties. According to the analysis, the shortcomings of the Spearman correlation method are due to non-additive interactions between the input variables. These produce uncertainties, whose source can be identified only with higher order methods such as the variance decomposition. We also compare the quantitative effectiveness of the variance decomposition to the Spearman correlation method, showing significant improvement. Using the evaluated total effects, we rank the input uncertainties with respect to their overall importance. We summarize the results of the paper in Section 6.

2. The fuel performance code FRAPCON

The fuel performance model used in this study is the FRAPCON-3.4 code that is maintained by the Pacific Northwest National Laboratory (Geelhood et al., 2011a,b). FRAPCON is a deterministic fuel performance code that calculates the steady-state response of light-water reactor fuel rods during long-term burn-up. Boundary conditions such as the power history and the coolant properties, in addition to the rod fabrication parameters, are supplied as input. The output of the code comprises several observables, including the fuel and cladding temperature distributions in the radial and axial directions, mechanical deformations of the pellet and the cladding, internal pressure, gap conductance, and so on. The physical phenomena described in the code include heat conduction through the fuel, gap and cladding into the coolant, fuel densification and swelling, cladding elastic and plastic deformations, fission gas release and cladding oxidation. The thermal and mechanical solutions are strongly coupled through the gap conductance, which is a function of, for example, pellet and cladding dimensions, and has a strong influence on the radial heat conduction. In addition to the gap conductance, the different submodels become interconnected via phenomena such as the fission gas release, which influences both the thermal and mechanical solutions through gap conductance and pressure and is itself affected by the fuel temperature.

The strong coupling between the different phenomena imply that the model is highly nonlinear and interactions between input variables are very likely. To analyze the output of such a model, we use the statistical methods described in Section 3, which involve Monte Carlo sampling of the input variables from given probability distributions. As FRAPCON is a deterministic code (one input producing exactly one deterministic solution), the sampling of input variables has to be done by external means. For this purpose we have developed a Python script that performs the sampling using methods discussed in Section 3 and generates the FRAPCON input files (Ikonen, 2012). The code is then run and the results post-processed on a Linux cluster.

3. Statistical analysis methods

3.1. General considerations

A fuel performance code is typically very complex, with dozens of input variables and several output observables of interest. In the analysis of such a complex system, determining the propagation of uncertainties from input to output can be a delicate task. Numerous alternative methods of uncertainty and sensitivity analysis exist, each having their advantages and disadvantages. Two ways to group different methods is to distinguish between deterministic and statistical methods, and local and global sensitivity analysis (Saltelli et al., 2008; Ionescu-Bujor and Cacuci, 2004; Cacuci and Ionescu-Bujor, 2004).

With deterministic methods, one estimates the response of the model output to the changes in the value of an input variable either by analytical means, or by deterministic sampling of individual values. With statistical methods, on the other hand, one samples the values of the input variables from a distribution and calculates the

response (output) of the model for each sampled value. The distribution of the output can then be analyzed with various statistical methods. Most of the deterministic methods are also local, meaning that the sensitivity of the output is measured in the neighborhood of a single point in the input variable space, typically varying only one variable at a time. With global sensitivity analysis one varies all the input variables at once, solving the model for each sampled combination of the variables.

For the purposes of this study, analytical and deterministic methods seem impractical. This is both due to the mathematical complexity of the system that is being studied, and the amount of labor that would be necessary in implementing analytical methods into a fuel performance code. However, since the code is very fast computationally (taking only a few seconds per model evaluation), evaluating the uncertainties and sensitivities by statistical sampling is efficient. In addition, we focus on global instead of local analysis methods, because they are better suited for describing the interactions between different input variables (Saltelli and Annoni, 2010). Specifically, the analysis is done using the Spearman correlation coefficients (Draper and Smith, 1998; Kvam and Vidakovic, 2007) and Sobol' variance decomposition (Sobol', 1993; Saltelli, 2002; Glen and Isaacs, 2012). The former represents a more standard method of sensitivity analysis in the nuclear engineering field, while the latter is a more advanced method that has recently asserted itself among practitioners of sensitivity analysis (see, *e.g.* Saltelli et al., 2010 and references therein).

Before describing the methods in detail, we start by defining the problem and the associated notations.

3.2. Preliminaries and problem definition

A model of a complex system can be represented as a mapping $Y = f(\mathbf{X})$, where Y is the output and $\mathbf{X} = [X_1, X_2, \ldots, X_{k-1}, X_k]$ is the vector of k input variables. Without any loss of generality, we may restrict our discussion to the case of a single output, Y. The uncertain value of each variable X_i is characterized by a probability distribution $\mathcal{P}_i(X_i)$, from which one can obtain the mean μ_i and the variance σ_i^2 of X_i. Here, we only consider distributions with finite μ_i and σ_i^2. In principle, the elements of $\mathbf{X}$ can be correlated, but in this work we consider the inputs of a fuel performance code uncorrelated. Hence, we will restrict our analysis to the case where the elements of $\mathbf{X}$ are independent.

In addition to determining the uncertainty in Y that arises from the uncertainty of $\mathbf{X}$, we wish to establish how the uncertainty of each variable X_i contributes to the uncertainty of Y. *Specifically, our goal is to find the proportion of the uncertainty (variance) of Y that is explained by the uncertainty (variance) of* X_i. Moreover, we wish to look at interactions, that is, the effect of changing more than one variable simultaneously. To do this, we first need to make a few formal definitions.

First, let us quantify the effect of changing just one variable, X_i. The linearized response in Y to the change in X_i is given by the partial derivative $\frac{\partial Y}{\partial X_i}$. However, the derivative alone does not take into account the uncertainty of different input variables: if the functional form of f is the same for X_i and X_j, the derivative will be the same regardless of the magnitude of σ_i or σ_j. However, the variable with the larger variance will cause a larger uncertainty in the output. Therefore, it is more practical to consider as a sensitivity measure the standard-deviation-normalized derivative

$$r_i^{\mathrm{lin}} = \frac{\sigma_i}{\sigma_Y}\frac{\partial Y}{\partial X_i}. \tag{1}$$

Here σ_Y denotes to standard deviation of Y and the superscript 'lin' in r_i^{lin} implies that this is a linearized sensitivity measure.

In practice, the derivative in Eq. (1) is evaluated numerically from a sample of size N by fitting. For linear regression, it can be shown that the least-squares-estimated angular coefficient $\hat{b}$ is related to the covariance $\mathrm{cov}(X_i, Y)$ of the variables X_i and Y as follows (Draper and Smith, 1998)

$$\frac{\sigma_i}{\sigma_Y}\hat{b} = \frac{\mathrm{cov}(X_i, Y)}{\sigma_i \sigma_Y} \equiv R_i. \tag{2}$$

The quantity R_i is the Pearson correlation coefficient. For a linear model, R_i is the statistical equivalent of the normalized derivative of Eq. (1). In addition, it can be shown that the square of R_i can be written as the ratio of the variance of the regression-fitted values and the variance of the original data (Draper and Smith, 1998). Thus, R_i^2 is the proportion of *variance explained* by a linear function of X_i.

As a sensitivity measure, R_i^2 is very limited. It can give a complete description of the propagation of uncertainties from $\mathbf{X}$ to Y only for a *linear* and *additive* systems. (A system is linear, if the function f is linear, and additive, if f can be written as a sum in which each term only depends on one variable X_i.) In such case, the sum $\sum_i^k R_i^2 = 1$. However, if the system is nonlinear or non-additive, a linear sensitivity measure can explain only part of the uncertainty of Y, so that $\sum_i^k R_i^2 < 1$. For this reason, improved sensitivity measures are needed to analyze nonlinear models.

3.3. Spearman correlation coefficients

A widely used extension of the Pearson R_i to nonlinear monotonic functions is the Spearman rank correlation coefficient ρ_i (Draper and Smith, 1998; Kvam and Vidakovic, 2007). The corresponding sensitivity measure ρ_i^2 has been widely used to classify correlations in data, also in nuclear engineering. It is also one of the GRS recommended methods of uncertainty and sensitivity analysis (Glaeser, 2008).

Mathematically, the Spearman ρ_i is a linear correlation calculated for ranks, not the data itself. To obtain the ranks x_i and y, the realizations of the variables X_i and Y are arranged into ascending order and assigned values from 1 to N. The correlation coefficient ρ_i is then calculated as (Kvam and Vidakovic, 2007)

$$\rho_i = \frac{\mathrm{cov}(x_i, y)}{\sigma_{x_i}\sigma_y}. \tag{3}$$

The rank correlation coefficient ρ_i can be used in the same manner as the Pearson R_i to obtain the sensitivity of the output Y to the input variables X_i, with ρ_i^2 giving an estimate of the contribution of the ith variable to the variance of Y. On nonlinear systems, the rank correlation method performs considerably better than the linear regression method. However, due to its construction, its ability to describe non-monotonic or non-additive models is limited (Sallaberry and Helton, 2006). For instance, for the simplest possible non-additive function $Y = f(X_1, X_2) = X_1 X_2$, with X_1 and X_2 normal and $\mu_1 = \mu_2 = 0$, one has the correlation coefficients $\rho_1 = \rho_2 = 0$, leaving all of the model's variance unexplained. In a fuel performance code, where such interactions between different input variables are important, the rank correlation coefficient may be an inadequate descriptor of the system. Therefore, more advanced methods need to be considered to study the effect of variable interactions.

3.4. Sobol' variance decomposition

3.4.1. Definition of the sensitivity indices

The variance decomposition method was first proposed by Sobol' (Sobol', 1993). The idea is to express the variance $V(Y)$ of the output as a finite sum, where each term corresponds to the

contribution of one input variable X_i or to the interaction of several input variables. The variance of Y is written as

$$V(Y) = \sum_{i}^{k} V_i + \sum_{i}^{k}\sum_{j>i}^{k} V_{ij} + \cdots + V_{12\ldots k}. \quad (4)$$

Here, V_i is the *first order effect* on the variance $V(Y)$ due to the variable X_i, V_{ij} the *second order effect* due to the interaction of X_i and X_j, and so on, up to $V_{12\ldots k}$, which is the kth order effect due to the interaction of all k input variables. Dividing both sides of Eq. (4) by $V(Y)$ gives

$$\sum_{i}^{k} S_i + \sum_{i}^{k}\sum_{j>i}^{k} S_{ij} + \cdots + S_{12\ldots k} = 1, \quad (5)$$

where $S_i \equiv V_i/V(Y)$ is the *first order sensitivity index*, $S_{ij} \equiv V_{ij}/V(Y)$ is the *second order sensitivity index*, and so on. The sum of all sensitivity indices up to kth order is one. Up to second order, the terms of the variance decomposition of Eq. (4) are $V_i = V(E(Y|X_i))$ and $V_{ij} = V(E(Y|X_i, X_j)) - V(E(Y|X_i)) - V(E(Y|X_j))$. Here the notation $E(Y|X_i)$ denotes the conditional expectation value of Y with fixed X_i. The variance of this expectation value, $V(E(Y|X_i))$ is then taken over the different values of X_i. The quantity V_i thus gives the contribution of X_i to the variance of Y, when the effect of all other variables is averaged out. However, V_i does not include any interaction effects of X_i with the other variables. The second order effect, V_{ij}, takes into account the interactions between two variables, X_i and X_j. Higher order terms are defined in a similar manner. Further discussion, along with illustrative examples, can be found, *e.g.*, in Chapters 1 and 4 of (Saltelli et al., 2008).

To make the connection with the previous discussion, let us look at the first order index S_i more closely. The index is defined as

$$S_i = \frac{V(E(Y|X_i))}{V(Y)}, \quad (6)$$

thus giving proportion of the variance caused by X_i in proportion to the total variance of Y. Therefore, in light of the discussion of Section 3.2, *for a linear model* it holds that $S_i = R_i^2$. The sensitivity index S_i is therefore a generalization of the linear regression correlation coefficient (or rather, its square). The variance decomposition method can therefore be used to extract the same information as linear regression (and more, as we will discuss), apart from the sign of the correlation, which is trivially obtainable.

Since S_i describes the additive (non-interacting) contribution of X_i to the variance of Y, the sum of the first order indices has an upper bound

$$\sum_{i}^{k} S_i \leq 1. \quad (7)$$

The equality is exact only for additive models, for which all the higher order indices are zero. However, nonlinearity does not imply break-down of the equality; the equality holds even for nonlinear systems, as long as the model is additive.

3.4.2. Total effect index

Measuring all the sensitivity indices up to kth order would explain all of the models variance. To do this in practice, however, would be a formidable computational task. Fortunately, it turns out that it is relatively inexpensive to estimate the so-called *total effect index*, T_i, which takes into account all the first-order and interaction effects of one variable X_i. The total effect index for variable X_i is defined as

$$T_i = \sum_{l}^{k} \delta_{il} S_l + \sum_{l}^{k}\sum_{m>l}^{k} (\delta_{il} + \delta_{im}) S_{lm} + \cdots + S_{12\ldots k}, \quad (8)$$

where δ_{ij} is the Kronecker delta. For example, for a three-variable model ($k = 3$), the total effect of variable X_1 is $T_1 = S_1 + S_{12} + S_{13} + S_{123}$.

The degree of non-additivity of the model with respect to input variable X_i can be characterized by the difference $T_i - S_i$. For additive models, having no interaction terms, this difference is equal to zero. On the other hand, for non-additive models the difference is positive:

$$T_i - S_i = 0 \,(\text{additive models}) \quad (9)$$

$$T_i - S_i > 0 \,(\text{non} - \text{additive models}) \quad (10)$$

A large difference signals the importance of interactions involving the variable X_i.

Since the second and higher order indices are included in the total effect indices of more than one variable, it holds that

$$\sum_{i}^{k} T_i \geq 1. \quad (11)$$

Again, the equality is exact for additive models.

3.4.3. Numerical implementation

Efficient evaluation of the Sobol' sensitivity indices has been studied considerably in the recent years (Saltelli et al., 2008, 2010; Glen and Isaacs, 2012; Jansen, 1999; Homma and Saltelli, 1996; Lilburne and Tarantola, 2009). The brute force method would use the bare definitions of the conditional variances to compute the indices. However, there are several more efficient approaches. Most of them rely on reducing the computational load by performing the random sampling in a very specific way, accomplished as follows.

First, two sets of random inputs are generated. The first set (the "sample") consists of Nk independent input values (N for each k inputs), used to solve the model N times. This gives N independent realizations of the output, $Y_{0,n}$, with $n = 1, 2, \ldots, N$ (the meaning of the subscript '0' will become apparent shortly). The same is then repeated for another independent set of random inputs (the "re-sample"), yielding another N independent solutions of the model. For the re-sampled outputs, we use the primed notation $Y'_{0,n}$. The sample and the re-sample inputs are then mixed to form k sets of inputs from the previously generated random numbers. This is done by taking all the input values from the sample set, except those corresponding to the input variable i, which are taken from the re-sample set. For each i, this gives a set of Nk input variables, which are again used to evaluate the model N times, giving the outputs $Y_{i,n}$. Here the subscript i is used to indicate the variable for which the re-sample set is used, with '0' signifying that no inputs from the re-sample are used. The mixing procedure is then repeated, this time using the re-sample set for all variables except one, and the sample set for the variable i. Evaluation of model with these inputs then gives the primed results, $Y'_{i,n}$. The whole procedure requires a total of $N(2k+2)$ model evaluations, the computational effort thus scaling linearly with the number of inputs k. For a more thorough discussion of the procedure, see, for instance, Chapter 4 of Saltelli et al. (2008), or Saltelli et al. (2010), Glen and Isaacs (2012).

Having obtained the outputs from the randomly sampled inputs, what remains is the calculation of the sensitivity indices. For this, there are many different formulas, each constructing the conditional variances in a slightly different way from the output combinations (for a recent review and comparison, see Glen and Isaacs, 2012). In this work, several different variants were assessed,

including those discussed in Saltelli et al. (2008, 2010), Saltelli (2002), Lilburne and Tarantola (2009), Jansen (1999). For the analyzed data, the method labeled 'D3' in Glen and Isaacs (2012) proved to be the most efficient one, giving the smallest errors with fixed N. The method subtracts spurious correlations (correlations caused by finite sample size in an ideally uncorrelated data) and uses double estimates for improved accuracy. The derivation of the method is described in Glen and Isaacs (2012).

The method is formulated using standardized output $Z_{i,n}$, defined as

$$Z_{i,n} = \left(Y_{i,n} - m_i\right)/\sqrt{v_i}, \tag{12}$$

where m_i is the mean $m_i = \frac{1}{N}\sum_n Y_{i,n}$ and v_i is the variance $v_i = \frac{1}{N}\sum_n Y_{i,n}^2 - M_i^2$. Analogous definition holds for the primed output. From the standardized data various correlations are then calculated. In the following, we drop the subscript n, so that $Z_i \equiv Z_{i,n}$, and the sum implies summation over n from 1 to N. The required correlations are

$$C_i = \frac{1}{2N}\sum\left(Z_0' Z_i + Z_0 Z_i'\right), \tag{13}$$

$$C_{-i} = \frac{1}{2N}\sum\left(Z_0 Z_i + Z_0' Z_i'\right), \tag{14}$$

$$P_i = \frac{1}{2N}\sum\left(Z_0 Z_0' + Z_i Z_i'\right), \tag{15}$$

$$C_{ai} = \frac{C_i - P_i C_{-i}}{1 - P_i^2}, \tag{16}$$

$$C_{a-i} = \frac{C_{-i} - P_i C_i}{1 - P_i^2}, \tag{17}$$

for the one-variable indices, and

$$C_{ij} = \frac{1}{2N}\sum\left(Z_i' Z_j + Z_i Z_j'\right), \tag{18}$$

$$C_{-ij} = \frac{1}{2N}\sum\left(Z_i Z_j + Z_i' Z_j'\right), \tag{19}$$

$$P_{ij} = \frac{1}{2N}\sum\left(Z_i Z_i' + Z_j Z_j'\right), \tag{20}$$

$$C_{aij} = \frac{C_{ij} - P_{ij} C_{-ij}}{1 - P_{ij}^2}, \tag{21}$$

$$C_{a-ij} = \frac{C_{-ij} - P_{ij} C_{ij}}{1 - P_{ij}^2}. \tag{22}$$

for the second-order indices. In the above the C's are the double estimate correlations, the P's the spurious correlations and the C_a's correlation estimates partly adjusted for spurious correlations.

The estimators for the sensitivity indices are then obtained as follows. The first-order index, or the main effect, is

$$S_i = C_j - P_j \frac{C_{a-i}}{1 - C_{ai} C_{a-i}}, \tag{23}$$

the total effect is

$$T_i = 1 - C_{-j} + P_j \frac{C_{a-i}}{1 - C_{ai} C_{a-i}}, \tag{24}$$

and the second order effect is

$$S_{ij} = C_{ij} - P_{ij} \frac{C_{a-ij}}{1 - C_{aij} C_{a-ij}} - S_i - S_j. \tag{25}$$

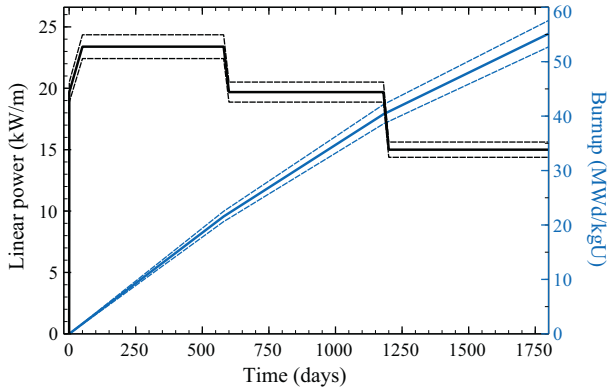

Fig. 1. Black lines, left axis: the power history (solid line) and its 95% confidence limits (dashed lines) used in the scenario. Blue lines, right axis: the resulting average burnup with the 95% confidence limits. (For interpretation of the references to color in this figure legend, the reader is referred to the web version of the article.)

3.5. Sampling of the input variables

The correlation coefficients and sensitivity indices can be calculated using pseudo-random numbers, quasi-random numbers or other methods to sample the input variable distributions. For quasi-random numbers, the input variable distributions can be calculated from the uniform distribution by numerical transform using the inverse cumulative distribution function (Press et al., 2002). In this work, the sampling was done with both pseudo-random and quasi-random numbers, using the Sobol' sequence (Sobol', 1967; Antonov and Saleev, 1979) to generate the latter, as recommended in the literature (Saltelli et al., 2008, 2010; Sobol', 1993). The quasi-random sampling showed slightly faster convergence, although no systematic study of the convergence rate was done. Hence, in the following Sections we show only the results obtained with the Sobol' sequence sampling of the input variables.

4. Scenario specifications and varied parameters

The analyzed scenario represents a hypothetical steady-state irradiation of a uranium oxide fuel rod in the Three Mile Island 1 (TMI-1) PWR reactor. The scenario is designed to bring the fuel rod to a relatively high burn-up of 50–60 MWd/kgU (depending on the input values), using a simplified power history shown in Fig. 1. The reactor power remains constant for several hundreds of days, with only two changes in the power level during the scenario. Since many of the measured quantities depend on the linear heat rate (LHR), such a simplification is in practice mandatory. The dependencies on the LHR can still be extracted by analyzing the uncertainty of the power history, and by looking at the changes that occur when the overall power level changes. The axial power profile is given in Table 1.

The relevant input parameters are reproduced in Table 2. The upper part of the table lists the fabrication and system parameters with their uncertainties, while the lower part lists the uncertainties in the material correlations, models and power history. For the fabrication parameters, the uncertainties reported in the OECD Benchmark for Uncertainty Analysis in Best-Estimate Modeling for Design, Operation and Safety Analysis of LWRs (UAM-LWR) (Blyth et al., 2012) have been used as a guideline. The uncertainties in the material correlations and computational models were determined

Table 1
The axial power profile of the scenario. Linear interpolation is used to obtain the power at the intermediate positions.

Position (mm)	0.0	304.8	609.6	914.4	2743.2	3048.0	3352.8	3657.6
Relative power	0.63	0.83	1.03	1.08	1.08	1.03	0.83	0.63

Table 2
The best estimate values of input parameters and their uncertainties (the 95% confidence interval) used in the analyzed scenario. If no uncertainties are indicated, the input was not varied. For the FRAPCON correlations and the power history (the bottom half of the table) only uncertainties are shown, since the best estimate value is a function of several variables or changes with time. The last column lists the abbreviation used for the varied input parameters in the figures of this paper.

Parameter	Value	Abbr.
Clad outer diameter	(10.92 ± 0.06) mm	clod
Clad thickness	(0.673 ± 0.025) mm	clth
Pellet outer diameter	(9.40 ± 0.02) mm	fuod
Total fuel height	3657.6 mm	–
Fuel pellet height	11.43 mm	–
Fuel enrichment (atom-%)	(4.85 ± 0.003)%	fuenrch
Density (% of theoretical)	(93.8 ± 1.6)%	fuden
Clad type	Zr-4	–
Fill gas type	Helium	–
Fill gas pressure	1207 kPa	–
Fuel rod pitch	14.43 mm	–
Coolant pressure	(15.51 ± 0.31) MPa	coolp
Coolant inlet temperature	(561 ± 3) K	coolt
Coolant mass flux	(3460 ± 69) kg/(m^{2}s)	coolmf
Fuel thermal conductivity	±10%	futc
Fuel thermal expansion	±15%	futex
FGR diffusion coefficient	+200%/-67%	Dfgr
Fuel swelling	±20%	fuswell
Clad creep	±30%	clcreep
Clad axial growth	±50%	clgrowth
Clad corrosion	±40%	clcor
Clad H concentration	±80 ppm	clhcon
Clad thermal conductivity	±5 W/mK	cltc
Clad thermal expansion	±30%	cltex
Gas thermal conductivity	±0.02 W/mK	gastc
Coolant heat transfer	±5%	coolhtc
Linear power	±5%	power

based on the data presented in a recent evaluation (Geelhood et al., 2009) and the recommendations given in the FRAPCON manual (Geelhood et al., 2011a,b). For all variables, the probability distribution is assumed Gaussian, with a cut-off at the lower and upper 2.5% percentiles. The input parameters are assumed mutually independent. For most inputs this assumption holds exactly, but for some only approximately. For instance, the rod's physical dimensions may become weakly correlated due to the manufacturing process. However, since data on such correlations is not available, the correlations are assumed negligible. For the power history, the same percentual deviation from the mean is used for each time step. Default FRAPCON-3.4 models are used in the code runs.

5. Results and discussion

5.1. General remarks

The scenario described in Section 4 was modeled with FRAPCON-3.4 using a Python script for sampling the input variable distributions and generating the FRAPCON input files. The distributions were sampled using the inverse cumulative distribution function method to transform the uniformly distributed Sobol' sequence quasi-random numbers into Gaussian numbers with the 2.5% upper and lower cut-offs. The sample size was $N = 50,000$ independent runs. In addition, for the Sobol' sensitivity indices, a re-sample of size $N = 50,000$ and 21 mixed samples of the same size (one for each input variable, as discussed in Section 3) were generated. The total number of performed FRAPCON runs was therefore 1.15×10^6, taking approximately 20 CPU-days on a Linux cluster.

The quantitative results of the analysis of course depend on the modeled scenario, parameter variations and the computational model. For example, increasing the variance of a single input parameter would increase its contribution in proportion to the others. Because of input interactions, simply scaling the results with the input's variance is not sufficient. Hence, the input variances should be chosen as realistic as possible for the analyzed scenario. In addition, the same analysis, repeated using a different fuel performance code, would give quantitatively different results due to the different underlying models. However, the trends discussed in this Section should be valid for steady state fuel behavior analysis in general.

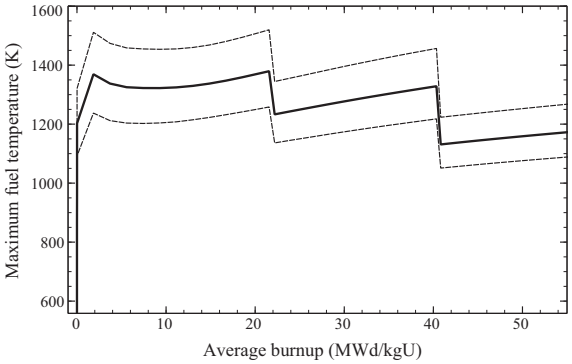

Fig. 2. The maximum fuel temperature (solid line) and its 95% confidence limits (dashed lines) as a function of burnup.

5.2. Average values and uncertainty analysis

Out of the sample of $N = 50,000$ independent runs, the average (mean) values were calculated for several outputs. The results for the maximum fuel temperature, average cladding temperature, rod internal pressure, axially averaged gap width and gap conductance, and the cladding radial displacement and hoop stress at the central axial node are shown in Figs. 2–9 . The uncertainties of the outputs were evaluated by calculating the upper and lower 2.5% percentiles (*i.e.*, the 95% confidence interval) from the modeled distribution. These are also shown in Figs. 2–9.

At the beginning of irradiation, the maximum fuel temperature climbs to almost 1370 K, as shown in Fig. 2. The temperature then goes down slightly as the conductivity of the fuel and the gap conductance improve as a result of pellet densification and reduction of the gap size. At slightly higher burnup, the temperature starts to increase as the accumulating fission products decrease the thermal conductivity of the fuel. The uncertainty of the temperature is significant, and remains roughly constant at ±130 K until the linear power is reduced, whereupon the uncertainty also decreases.

The mean cladding temperature behaves very similarly to the fuel temperature, slowly increasing with burnup and decreasing with decreasing power (see Fig. 3). The uncertainty remains quite

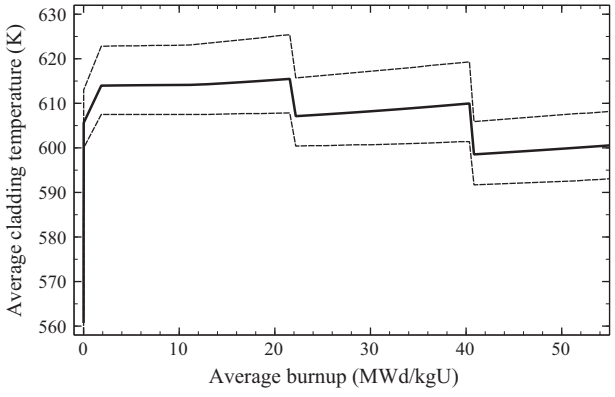

Fig. 3. The average cladding temperature (solid line) and its 95% confidence limits (dashed lines) as a function of burnup.

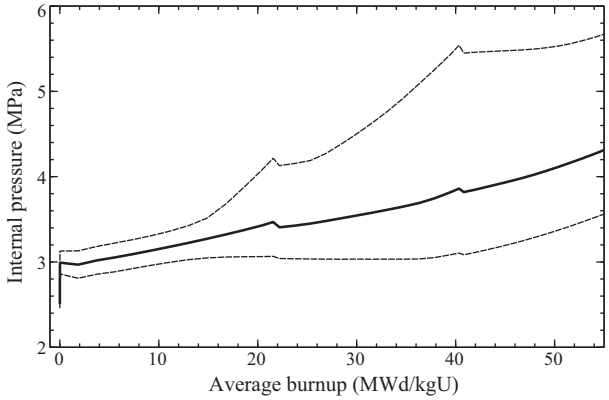

Fig. 4. The internal rod pressure (solid line) and its 95% confidence limits (dashed lines) as a function of burnup.

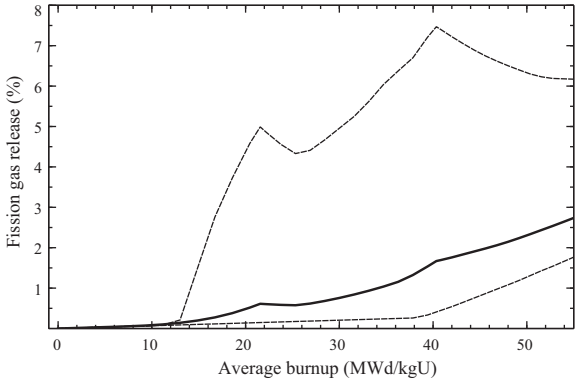

Fig. 5. The average amount of released fission gas (solid line) and its 95% confidence limits (dashed lines) as a function of burnup.

stable at ±8 K. However, even though the behavior looks very similar to the fuel temperature, the sensitivity analysis will reveal that the uncertainties in the fuel and cladding temperatures are dominated by completely different input uncertainties.

The internal pressure of the rod (Fig. 4) and the fission gas release (Fig. 5) behave very similarly, the time evolution of the FGR determining the evolution of the pressure to a large degree. With increasing amount of released fission gases, the pressure rises steadily with burnup. At the end of the irradiation, the average FGR amounts to roughly 2.7%, with the pressure reaching 4.3 MPa. The uncertainty in both is very high, and typically increases

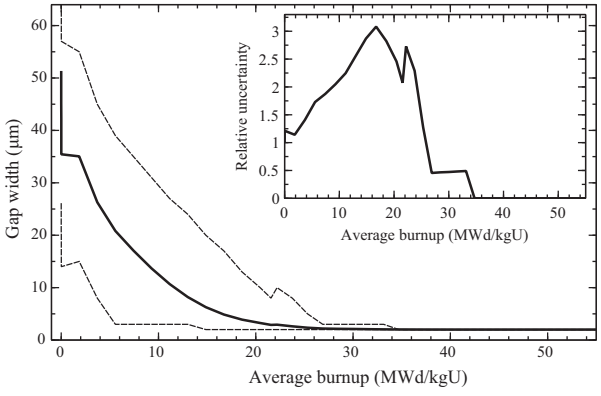

Fig. 6. Main plot: the average gap width (solid line) and its 95% confidence limits (dashed lines) as a function of burnup. Inset: the relative uncertainty of the gap width in proportion to the mean gap width.

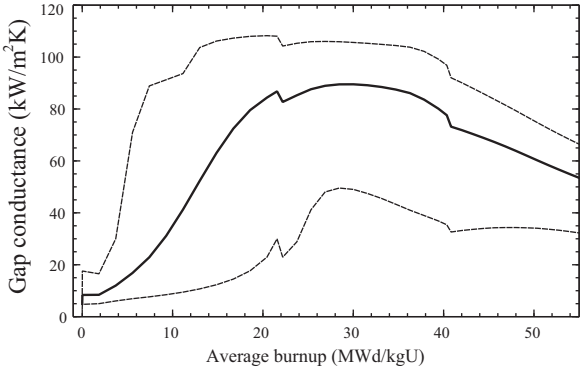

Fig. 7. The average gap conductance (solid line) and its 95% confidence limits (dashed lines) as a function of burnup.

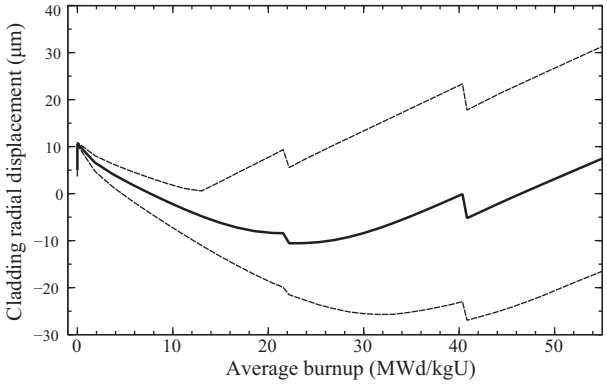

Fig. 8. The radial displacement of the cladding at the central axial node (solid line) and its 95% confidence limits (dashed lines) as a function of burnup.

with burnup. At the burnup of 40 MWd/kgU, the 95% confidence interval encompasses FGR amounts of 0.4% and 7.4%, and pressures between 3.1 MPa and 5.5 MPa.

The width of the pellet-cladding gap, shown in Fig. 6, is one the most important quantities to look at in the analysis of the fuel rod. At small burnup, the gap remains open, but eventually closes due to inward cladding creep and irradiation swelling of the fuel. This evolution of the gap width has a strong influence on the conductance of heat from the fuel to the cladding, and eventually leads to pellet-cladding interaction. In the present scenario, the gap remains almost completely open until the burnup of approximately 6 MWd/kgU, when it starts to close. Depending on the realization of the input variables, the gap has a fairly high probability of being open until about 25 MWd/kgU, and finally

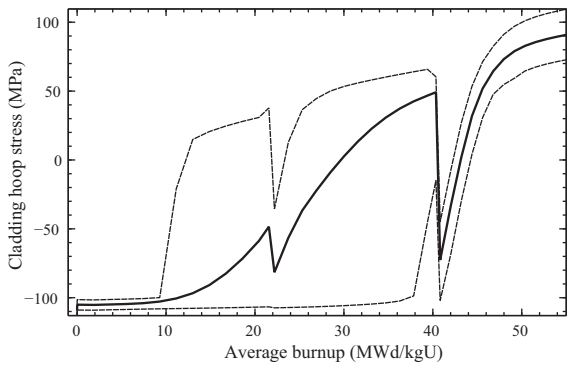

Fig. 9. The cladding hoop stress at the central axial node (solid line) and its 95% confidence limits (dashed lines) as a function of burnup.

closes in all the observed cases at approximately 40 MWd/kgU. The absolute uncertainty of the gap width decreases almost linearly with increasing burnup. However, the relative uncertainty (the width of the 95% confidence regime in proportion to mean gap width) behaves non-monotonically, first increasing with burnup and reaching its maximum of about 3 times the mean gap width at 16 MWd/kgU, then decreasing to zero as the gap closes.

The width of the gap and its uncertainty are reflected in the gap conductance (see Fig. 7). The conductance starts at a fairly modest mean value of 5 kW/m^{2}K, but increases beyond 80 kW/m^{2}K as the gap closes. The uncertainty also increases steeply, having its peak of about 94 kW/m^{2}K (between the lower and upper limits of the 95% tolerance) at the burnup of 15 MWd/kgU. It should be noted that this maximum uncertainty is much larger than is often assumed in non-fuel-specific modeling. From 20 to 35 MWd/kgU, the conductance remains close to 80 kW/m^{2}K. Towards higher burnups, the conductance again decreases due to the released fission gases into the gap, which decreases the overall conductance even when the pellet and the cladding are in mechanical contact. The effect of pellet-cladding interface pressure has also an effect on gap conductance when the gap is closed.

The radial displacement of the cladding is shown in Fig. 8. Initially, the cladding expands due to increasing temperature at rise to power. The cladding then begins to creep inwards because of the pressure difference. As the pellet comes into contact with the cladding, the direction changes and the cladding is pushed outward. This results in a bifurcation of the solutions into two groups. In one, the gap is closed and the cladding expands, while in the other the gap remains open and cladding continues to creep inward. As a result, the apparent uncertainty of the radial displacement increases strongly with burnup. The same is true for the cladding hoop stress, as shown in Fig. 9. Both the hoop stress and the radial displacement have very high uncertainties mid-scenario, at burnups of 20–40 MWd/kgU. As the gap closes after 40 MWd/kgU, the uncertainty in the hoop stress is dramatically reduced. For the radial displacement, which is accumulated over time, the large uncertainty remains even after gap closure.

5.3. Spearman correlation coefficients

As discussed in Section 3.3, a method that is often used to characterize the uncertainty and sensitivity of the output, is the calculation of correlation coefficients and, in particular, the Spearman rank correlation coefficient. Despite its inability to cope with non-additive terms, the Spearman correlation coefficient is still widely used because it is simple to implement in an analysis software and can be evaluated at relatively modest computational effort. It is also the sensitivity measure recommended by, for example, GRS (Glaeser, 2008).

We have used the sample of 50,000 independent runs to evaluate the Spearman correlation coefficients ρ between all the input-output pairs for different burnups. Since it would be cumbersome to present the data exhaustively, we focus only on the central findings. A snapshot of the correlation coefficients for the most important input variables at the burnup of 22 MWd/kgU is shown in Fig. 10. The same figure also visualizes the correlations between the input and output uncertainties in the form of scatter plots.

The first observation from the data is that the sensitivity to the input variables depends on the output. This is rather obvious, since the physical phenomena governing the response to the input are different for each output observable. Second, the thermal-mechanical behavior of the fuel rod is strongly influenced by the rod's burnup. Hence, the sensitivities to the input uncertainties also vary greatly with time and accumulated burnup. This important aspect will be discussed more closely in Section 5.4. Without going to specifics, we can however outline some general trends. For example, the coolant properties (temperature and pressure) tend to be most important for fresh rods, losing their relative importance as other factors come into play. Similarly, the pellet and cladding fabrication uncertainties tend to be most important for fresh and moderate-burnup rods (up to, say, 20 MWd/kgU). For higher burnups, the release of fission gases begins to dominate the uncertainties in many cases, along with the material properties such as the fuel thermal conductivity and expansion. However, because of the response to the inputs is different for each output, it is impossible to give any precise universal rules.

Table 3
The proportion of variance explained by additive contributions to the output variance, as given by $\sum_i^k \rho_i^2$ for different burnups (in MWd/kgU). The output abbreviations stand for (from left to right): gap conductance, internal pressure, maximum (fuel) temperature, average cladding temperature, cladding radial displacement at the central axial node, cladding hoop stress at the central axial node, and fission gas release.

Burnup	gapcon	intpr	tmax	tclav	cldr	hoopstrs	fgr
0.01	0.96	0.95	0.95	0.86	0.94	0.94	0.99
5.5	0.95	0.95	0.96	0.87	0.99	0.94	0.99
22	0.65	0.74	0.97	0.93	0.70	0.68	0.74
38	0.68	0.75	0.98	0.96	0.96	0.86	0.74
49	0.76	0.77	0.98	0.96	0.96	0.89	0.76

An important question is then, how well does the Spearman ρ explain the uncertainty of the output? As was discussed in Section 3.3, by construction the Spearman correlation coefficient can measure only the additive contributions to the output variance. However, we expect that the fuel behavior model will have complex non-additive interactions between various input parameters. To quantify the methods performance, we have calculated the sum $\sum_i^k \rho_i^2$ over the input variables X_i. For completely explained variance, the sum would be unity. A smaller value tells that part of the variance cannot be assigned to any of the input uncertainties. The results for different output observables at different times are gathered in Table 3. For low burnup, typically more than 95% of the variance is explained by the Spearman ρ.

With accumulated burnup, however, the sensitivity measure becomes significantly worse. Depending on the output, even as much as one third of the variance remains unexplained. For instance, at the burnup of 22 MWd/kgU, only 65% of the uncertainty in the gap conductance can be traced back to its source. For the remaining 35%, corresponding to the uncertainty of 28 kW/m^{2}K (cf. Fig. 7), the inputs responsible for the uncertainty cannot be identified. Thus, relying solely on the evaluation of ρ in sensitivity analysis can lead to serious lack of knowledge about the propagation of uncertainties.

5.4. Variance decomposition

5.4.1. General features and burnup dependence

To improve the results obtained with the Spearman correlation coefficients, the first order (S_i), second order (S_{ij}), and the total effect (T_i) sensitivity indices were evaluated from the sampled and re-sampled data of size $N = 50,000$. To calculate the averages, the sampling methods and estimators accounting for spurious correlations described in Section 3.4.3 were used. The statistical error was estimated by dividing the sample and the re-sample into 10 subgroups each, after which the averages were estimated independently for each subgroup. The estimate for the standard error was then calculated from the obtained averages. Such a bootstrapping method provides the averages as well as their error estimates without increasing the computational requirements (Archer et al., 1997).

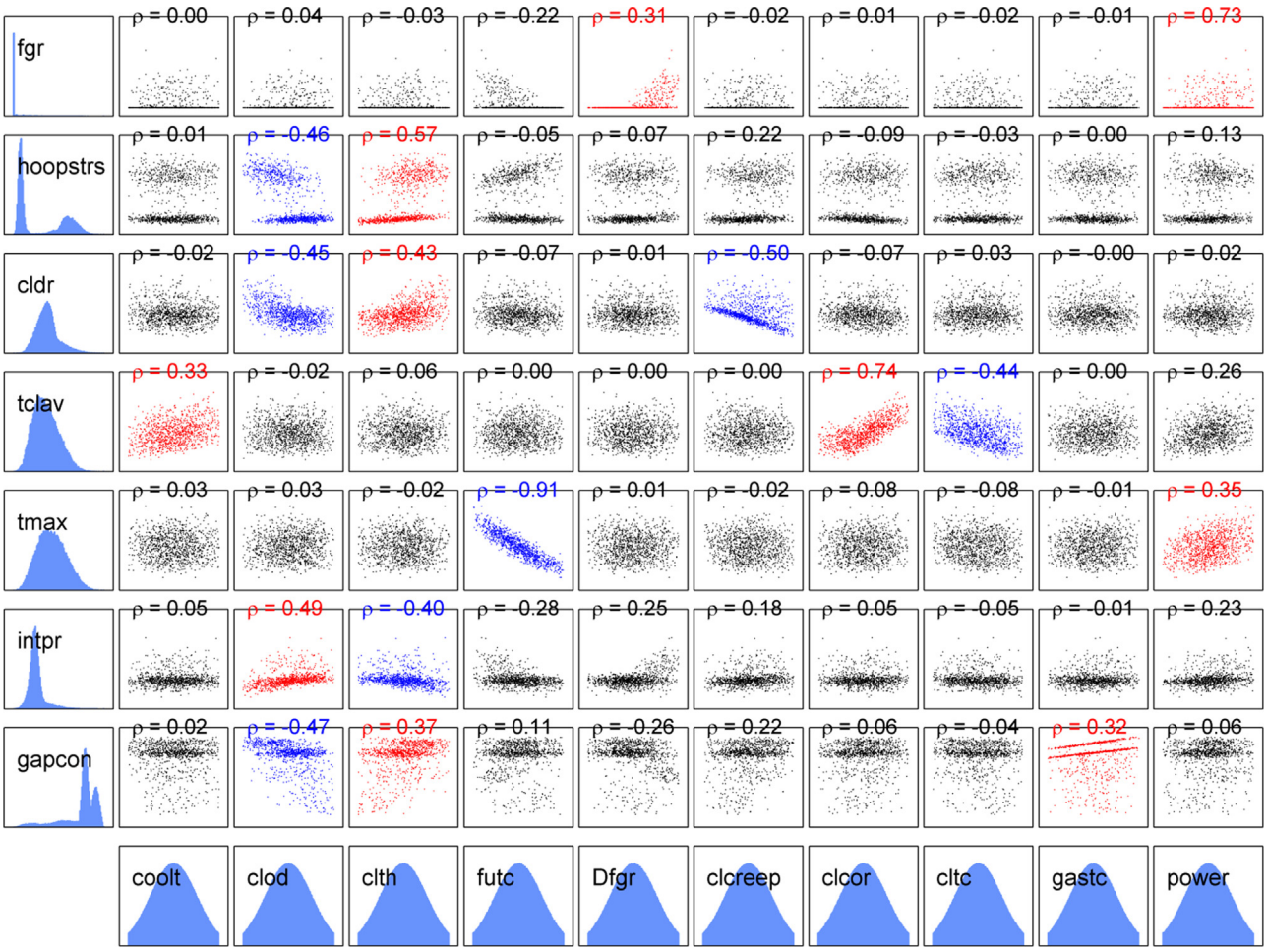

Fig. 10. Spearman correlation coefficients between the output and the most important input variables at the burnup of 22 MWd/kgU. The left column and the bottom row show the shape of the distribution of the output and input, respectively, while the middle part shows the scatter plots of the output as a function of the input variable. Here strong positive correlation is indicated with red color, and negative with blue color. For absolute values of the output and input, refer to Figs. 2–9 and Table 2. For the explanation of the inputs' abbreviations, refer to Table 2. The output abbreviations are the same as in Table 3. (For interpretation of the references to color in this figure legend, the reader is referred to the web version of the article.)

The first order and total effect indices evaluated for various output are shown in Figs. 11–18. The figures show the indices for the most important inputs as a function of burnup. In general, the importance of a given input depends not only on the considered output, but also on burnup. The results are consistent with the findings of the Spearman correlation coefficient analysis. Qualitatively, the ranking of the inputs by their importance is also very similar with both methods. However, important quantitative differences arise because of non-additive interactions between the inputs.

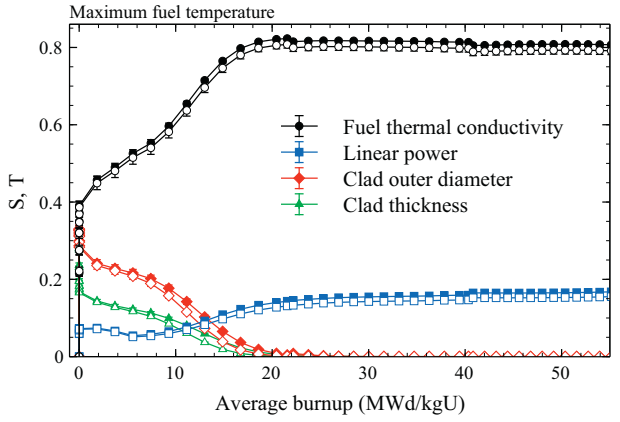

Fig. 11. Sobol' sensitivity indices for the maximum fuel temperature as a function of burnup. Open symbols correspond to the first order effects (S_i), while the closed symbols correspond to the total effect indices (T_i). Error bars indicate the 95% confidence limits.

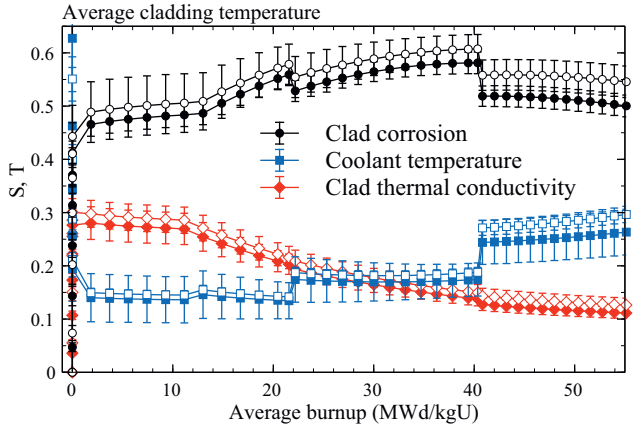

Fig. 12. Sobol' sensitivity indices for the cladding average temperature as a function of burnup. Conventions as in Fig. 11.

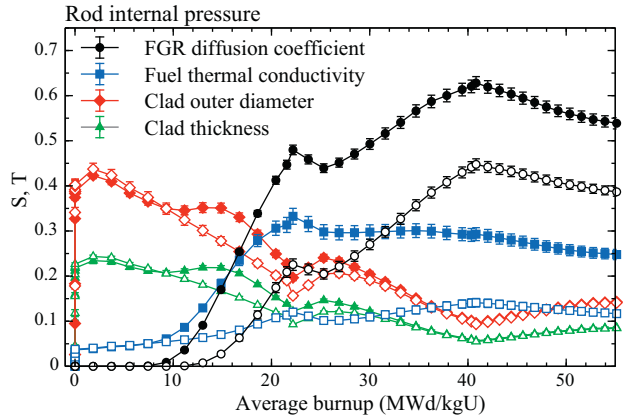

Fig. 13. Sobol' sensitivity indices for the rod internal pressure as a function of burnup. Conventions as in Fig. 11.

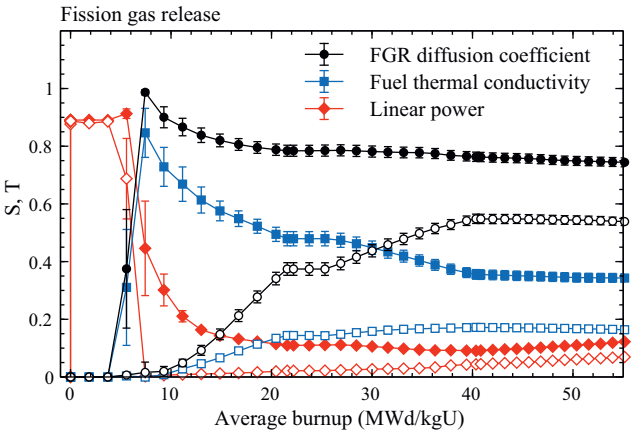

Fig. 14. Sobol' sensitivity indices for the fission gas release as a function of burnup. Conventions as in Fig. 11.

5.4.2. *Additivity of the outputs*

Based on the discussion of Section 5.3 and the results shown in Table 3, we expect that, for example, the maximum fuel temperature is an *additive* function of the inputs (irrespective of burnup). This means that, according to Eq. (9), the values of the indices S_i and T_i should be equal for any given i. As shown in Fig. 11, this is indeed the case. The figure shows the first order and total effect indices for the fuel thermal conductivity, average linear heat rate, and cladding outer diameter and thickness as a function of burnup. Independent of burnup, the indices agree within the statistical uncertainty, which shows that the maximum temperature is an additive function of the inputs and explains the good performance of the Spearman correlation coefficient.

As an opposite example, we may take the rod internal pressure. According to Table 3, for low burnup the Spearman correlation coefficient explains about 95% of the variance, which indicates

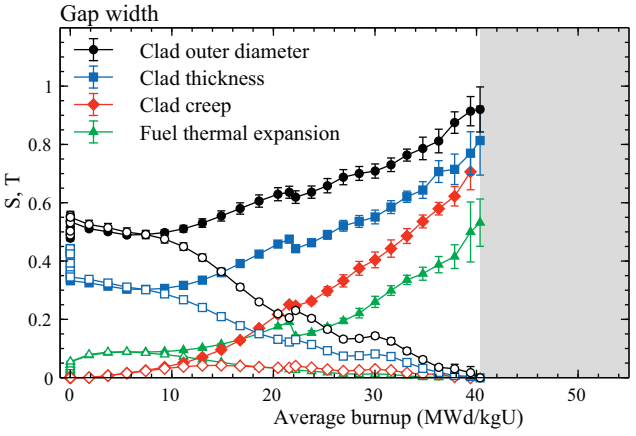

Fig. 15. Sobol' sensitivity indices for the gap width as a function of burnup. Evaluation of the indices beyond the burnup of approximately 40.4 MWd/kgU (indicated by the shaded area) is not possible because the gap is fully closed. Other conventions as in Fig. 11.

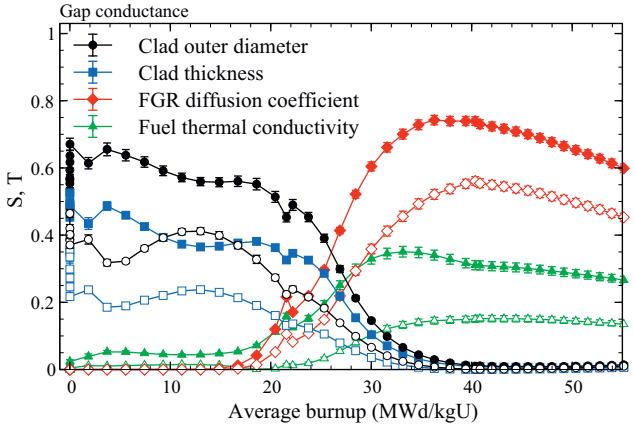

Fig. 16. Sobol' sensitivity indices for the gap conductance as a function of burnup. Conventions as in Fig. 11.

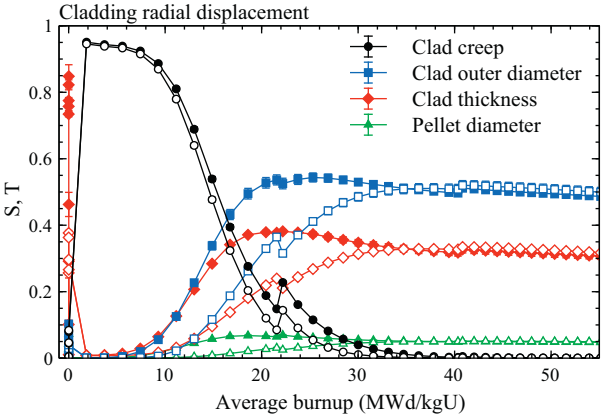

Fig. 17. Sobol' sensitivity indices for the cladding radial displacement at the center node as a function of burnup. Conventions as in Fig. 11.

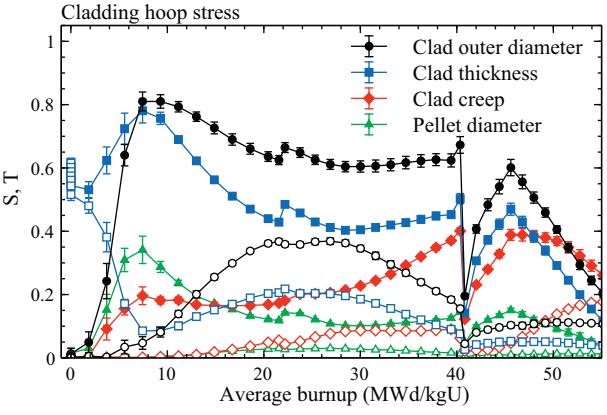

Fig. 18. Sobol' sensitivity indices for the cladding hoop stress at the center node as a function of burnup. Conventions as in Fig. 11.

near-additive behavior. However, at the burnup of 22 MWd/kgU and beyond, only about 75% of the variance is explained, suggesting non-additivity of the output. Looking at Fig. 13, the transition is clearly seen. Below 10 MWd/kgU, the first order and total effects indices are the same, diverging for higher burnup. Especially the indices linked to the FGR diffusion coefficient and fuel thermal conductivity display non-additivity, the total effects being about 0.15 higher than the first order effects.

Similar transitions between regions characterized by additive behavior and non-additive interactions can be seen for most of the outputs. The transition can also happen more than once, as for the cladding radial displacement (see Fig. 17), where the first order and total effect indices first diverge at the burnup of approximately 10 MWd/kgU, and then merge after 30 MWd/kgU.

Physically, at least two sources of the transitions can be identified. The first one is the introduction of new phenomena with increasing burnup. These phenomena can be either switched on by some criterion, or become gradually more important due to irradiation-induced mechanical and material changes. For example, the fission gas release (FGR) is unimportant at low burnup because the small amount of accumulated fission products in the fuel and their low fractional release into the gas gap. At moderate and high burnup, on the other hand, FGR has major influence on the rod internal pressure and gap conductivity. Since the FGR itself is strongly non-additive function of its inputs (especially the associated diffusion coefficient and the fuel thermal conductivity, as shown in Fig. 14), the non-additivity is transferred onward to other outputs. For example, the non-additivity of the internal pressure at burnups beyond 10 MWd/kgU is almost exclusively due to the coupling to FGR (see Fig 13).

The second major factor contributing to the transition between additivity and non-additivity is the evolution of the pellet-cladding gap. At low burnup the gap is open and the directly affected observables (internal pressure, cladding radial displacement and the gap width itself, see Figs. 13, 15 and 17) are additive. With accumulating burnup, the gap starts to close, with the exact moment depending statistically on the input values. The probability that the gap is closed quickly increases after 8 MWd/kgU, becoming almost certain around 30 MWd/kgU (see Fig. 6). In this intermediate regime, the statistical average of the outputs is taken over both the open and closed gap cases. The two cases are governed by completely different mechanical solutions, which gives rise to increased interaction between the inputs. This is reflected in Figs. 13, 15 and 17 by the difference between the first order indices and the total effect indices. For the cladding radial displacement and the internal pressure, the behavior becomes additive after the gap is completely closed at 34 MWd/kgU (apart from the contribution of the FGR). For the gap width, the simple additive behavior is never recovered. In fact, the behavior becomes progressively less additive, with 13 out of the 22 total effect indices having at least 10% influence on the variance of the gap width at 38 MWd/kgU. Although further analysis of uncertainty propagation in such a case would be extremely difficult, it is of little practical importance since the overall variance of gap width beyond 35 MWd/kgU is negligible.

As an important observation, we note that, according to Fig 16, the gap conductance is a non-additive function of the inputs throughout the scenario. At low to moderate burnups, the uncertainty is mostly attributed to the rod fabrication uncertainties, cladding outer diameter and thickness in particular. Because the gap conductance model itself is a non-additive function of the gap width (Geelhood et al., 2011a), the behavior is non-additive even for fresh fuel. After approximately 20 MWd/kgU, the dominant source of uncertainty is the FGR, with the model's diffusion coefficient being the most important source of uncertainty, followed by the uncertainty of the fuel thermal conductivity.

5.4.3. Performance of the variance decomposition

In Section 5.3, we evaluated the Spearman correlation coefficients for the gap conductance. At the burnup of 22 MWd/kgU, the sum of ρ_i^2 over all the inputs i was 0.65, as shown in Table 3. This result is very similar to what is obtained with the first order Sobol' indices. For the gap conductance at 22 MWd/kgU, the indices sum to $\sum_i S_i = 0.6$, which is of course no improvement over the Spearman coefficients.

However, the real advantage of the variance decomposition comes from the ability to quantify the interactions between input variables. For this purpose, the terms in the variance decomposition can be used in different combinations. For example, one may take the into account all the first order (S_i) and second order (S_{ij}) indices. For the gap conductance at 22 MWd/kgU, the sum

Table 4
The highest sensitivity of the output observables (top row) to the input variables (left column) during the scenario. The numbers in parentheses indicate the highest values of the total effect index T_i evaluated over the whole scenario for the particular input/output pair. The preceding number indicates the highest rank obtained during the scenario, with, *e.g.*, a "2." indicating that the particular variable has the second largest T_i at some point in the scenario, but never the largest one. The inputs are ordered by importance based on the ranking described above. For the abbreviations, refer to Tables 2 and 3.

Input	gapcon	intpr	tmax	tclav	cldr	hoopstrs	fgr
clod	1. (0.67)	1. (0.42)	1. (0.33)	8. (0.00)	1. (0.54)	1. (0.81)	3. (0.64)
Dfgr	1. (0.74)	1. (0.63)	6. (0.00)	12. (0.00)	11. (0.00)	10. (0.03)	1. (0.99)
clth	2. (0.53)	2. (0.23)	2. (0.28)	6. (0.00)	1. (0.85)	1. (0.78)	4. (0.52)
futex	3. (0.18)	1. (0.46)	5. (0.04)	10. (0.00)	4. (0.21)	1. (0.41)	4. (0.37)
clcreep	3. (0.21)	6. (0.05)	6. (0.02)	17. (0.00)	1. (0.95)	1. (0.40)	7. (0.06)
futc	2. (0.35)	2. (0.33)	1. (0.82)	11. (0.00	7. (0.06)	2. (0.36)	2. (0.85)
power	3. (0.14)	4. (0.11)	2. (0.17)	4. (0.07)	4. (0.13)	5. (0.16)	1. (0.91)
clcor	6. (0.03)	5. (0.12)	4. (0.01)	1. (0.58)	2. (0.39)	3. (0.12)	7. (0.01)
fuswell	8. (0.05)	11. (0.01)	11. (0.00)	16. (0.00)	3. (0.08)	1. (0.38)	11. (0.00)
coolt	7. (0.02)	5. (0.06)	5. (0.05)	1. (0.86)	3. (0.47)	6. (0.06)	6. (0.00)
coolp	5. (0.05)	2. (0.24)	7. (0.01)	9. (0.00)	2. (0.81)	2. (0.32)	7. (0.00)
cltc	8. (0.01)	9. (0.01)	5. (0.01)	2. (0.28)	2. (0.34)	9. (0.03)	5. (0.03)
fuden	5. (0.02)	7. (0.02)	3. (0.02)	9. (0.00)	8. (0.03)	9. (0.03)	2. (0.15)
fuod	3. (0.13)	4. (0.05)	5. (0.03)	10. (0.00)	3. (0.07)	3. (0.34)	3. (0.19)
gastc	4. (0.14)	9. (0.00)	7. (0.01)	21. (0.00)	13. (0.02)	10. (0.01)	9. (0.04)
fuenrch	16. (0.00)	16. (0.00)	15. (0.00)	12. (0.00)	17. (0.00)	16. (0.00)	4. (0.00)
coolmf	12. (0.00)	13. (0.00)	9. (0.00)	6. (0.00)	11. (0.05)	13. (0.01)	5. (0.00)
coolhtc	12. (0.00)	12. (0.00)	8. (0.00)	5. (0.01)	8. (0.08)	12. (0.01)	14. (0.00)
clgrowth	15. (0.00)	7. (0.02)	15. (0.00)	18. (0.00)	16. (0.00)	14. (0.01)	12. (0.00)
clhcon	20. (0.00)	20. (0.00)	20. (0.00)	19. (0.00)	20. (0.00)	20. (0.00)	17. (0.00)
cltex	21. (0.00)	21. (0.00)	21. (0.00)	20. (0.00)	21. (0.00)	21. (0.00)	19. (0.00)

of the second order indices is $\sum_i \sum_{j<i} S_{ij} = 0.28$, giving a total of 0.88 with the S_i's. Another way is to take the total effect of one variable X_i, and the first order effects of all other variables. This takes into account the first order effects of all variables and the interactions terms that involve the variable X_i. For example, one may choose the total effect of the cladding outer diameter, $T_{\mathrm{clod}} = 0.50$, and the first order effects $\sum_i S_i - S_{\mathrm{clod}} = 0.36$. This partition would bring the total to 0.86. In addition, one can take into account the second order effects *not* involving the cladding outer diameter (since these are already accounted for in T_{clod}). In this case, the most significant second order indices are $S_{\mathrm{futc,Dfgr}} = 0.057$, $S_{\mathrm{clth,clcreep}} = 0.0175$, $S_{\mathrm{Dfgr,power}} = 0.011$, $S_{\mathrm{futc,power}} = 0.0074$, $S_{\mathrm{clth,futex}} = 0.0074$ and $S_{\mathrm{clth,power}} = 0.0072$. Including these in the calculation takes the sum to 0.97.

This is a remarkable improvement from the Spearman ρ: instead of 35%, only 3% of the variance remains unaccounted for. Even the missing 3% can be tracked down by including the remaining second order terms in the calculation, which brings the overall sum to 1.00.

5.4.4. Ranking of the input variables

Finally, we should assess the question of the relative importance of the input uncertainties. As discussed above and shown in Figs. 11–18, the importance depends on the considered output and burnup. Therefore it is not possible to specify an input that universally ranks as the most important. However, some of the inputs appear to have significant impact on more than one output, and thus should rank high in importance, while others have virtually no influence on any of the outputs at all.

To simplify the matter, we have done the following. For each input and output, we have looked at the total effect indices (T_i) over the whole simulated scenario, collecting two sets of statistics. First, we have taken the maximum rank the input has for the given output. For example, if the input has the highest T_i for any nonzero burnup, the maximum rank will be one. Because the inputs' importances change with burnup, more than one input may have the same maximum rank. In addition, we have gathered the maximum values of T_i for nonzero burnup in the scenario.

The maximum ranks and values are shown in Table 4 for each varied input and for the most important outputs. The inputs are ordered so that on the top is the one with most number one ranks, followed by the one with second to most number one ranks, and so on. Although the ordering is somewhat arbitrary, it allows to quickly distinguish those inputs with significant contributions to the uncertainty of *some output at some point in the scenario* from the insignificant ones. In particular, since the total effect index is used for the evaluation, one can quickly discard the bottom ones as having almost no effect on the output. For example, in future analyses, it would be quite safe to consider the cladding thermal expansion (cltex in Table 4) as precise input, since its total effect to the overall variance of any of the considered outputs at any burnup between 0 and 55 MWd/kgU is less than 1%.

On the basis of Table 4, the input variables with the most broad impact on the uncertainties of the model's results are the cladding outer diameter, the diffusion coefficient of the fission gas release model, cladding thickness, fuel thermal expansion, cladding creep correlation, fuel thermal conductivity and the average linear heat rate. However, 15 out of the 21 inputs contribute significantly (by more than 10%) to the total variance of some output at some value of burnup. This result highlights the complexity of the system and demonstrates its sensitivity to the input values.

6. Conclusions

A hypothetical scenario of steady state irradiation of a TMI-1 fuel rod has been modeled with the FRAPCON-3.4 code. The uncertainties in input variables have been taken into account by Monte Carlo sampling from probability distributions, and extensive modeling of the different realizations has been done. The propagation of uncertainties has been analyzed using both the Spearman correlation coefficient method, which is conventionally used in the field, and by evaluating the first order, second order and total effect Sobol' sensitivity indices. The Sobol' variance decomposition is shown to perform significantly better in cases where non-additive interactions between input variables are present. This includes practically all the analyzed cases, with the exception of maximum fuel temperature and average cladding temperature. For example, in identifying the sources of uncertainty for the gap conductance at moderate burnup (22 MWd/kgU), the variance decomposition method can identify practically 100% of the input's contributions, while the Spearman correlation method only explains 65% of the output variance in the analyzed scenario.

The results suggests that first order sensitivity analysis methods should be used with caution in fuel performance modeling. With the possible exception of fuel centerline and cladding temperatures, the analysis should be complemented with higher order methods that take into account input interactions.

The interactions of the inputs and the necessity for higher order methods stem from the complexity of the system. For the same reason, identifying a single dominant source of uncertainty is not possible. The relative importance of the inputs depends not only on the considered output, but also on burnup. For instance, out of the 21 considered inputs, 15 have a contribution larger than 10% to the uncertainty of some output at some point in the scenario. In addition to complicating the analysis, this fact also makes it difficult to rule out inputs as a source of output uncertainty.

However, some fairly consistent trends can be identified. The inputs affecting the gap width, and thus gap conductance, rank among the most important ones. These are the as-fabricated cladding dimensions, cladding creep, fuel thermal expansion and, to some degree, the as-fabricated pellet diameter. Mostly the fabrication parameters influence the uncertainties at low burnup, with the other inputs becoming more important later in the rod's life, although for the cladding radial displacement the situation is reversed. Other important uncertainty sources are the diffusion coefficient in the FGR model, fuel thermal conductivity and linear power. The ranking of the inputs is very similar to that obtained in other sensitivity studies of the fuel rod (Christensen et al., 1981; Wilderman and Was, 1984; Boulore et al., 2012), although the present study identifies the FGR-related uncertainties among the most important ones. However, because FGR is a highly non-additive function of its inputs, it is easy to underestimate its contribution with first-order methods.

In addition to FGR, the evolution of the pellet-cladding gap with changing burnup is identified as one of the main sources involved in the burnup dependency of the sensitivity indices. Since the open gap and closed gap cases are governed by different physical models, the closure of the gap has a big influence on many of the sensitivity indices. In addition, the burnup regime where the gap is in the process of closing (*i.e.*, has a significant probability for both the open and closed states) is observed to have increased interaction between the inputs, caused by the mixing of the two states of the gap. Since the intermediate burnup regime is also an important regime of operation of nuclear reactors, this highlights the importance of using appropriate, higher order methods in the sensitivity analysis of the nuclear fuel rod.

Acknowledgements

This work was funded by SAFIR2014, the Finnish Research Programme on Nuclear Power Plant Safety 2011–2014.

References

Antonov, I., Saleev, V., 1979. An economic method of computing LP_τ-sequences. USSR Comput. Math. Math. Phys. 19, 252–256.

Archer, G., Saltelli, A., Sobol, I., 1997. Sensitivity measures, ANOVA-like techniques and the use of bootstrap. J. Stat. Comput. Simulat. 58, 99–120.

Bailly, H., Menessier, D., Prunier, C. (Eds.), 1999. The Nuclear Fuel of Pressurized Water Reactors and Fast Neutron Reactors. Lavoisier Publishing.

Blyth, T., Avramova, M., Ivanov, K., Royer, E., Sartori, E., Cabellos, O., 2012. Benchmark of uncertainty analysis in modeling (UAM) for design, operation and safety analysis of LWRs, Volume II: Specification and support data for the core cases (Phase II) [draft version 1.0]. Technical Report NEA/NSC/DOC(2012)? Nuclear Energy Agency.

Boulore, A., Struzik, C., Gaudier, F., 2012. Uncertainty and sensitivity analysis of the nuclear fuel thermal behavior. Nucl. Eng. Des. 253, 200–210.

Cacuci, D., 2010. Handbook of Nuclear Engineering. Springer.

Cacuci, D., Ionescu-Bujor, M., 2004. A comparative review of sensitivity and uncertainty analysis of large-scale systems – II: Statistical methods. Nucl. Sci. Eng. 147, 204–217.

Christensen, R., Eilbert, R., Rohrer, R., Was, G., 1981. Adjoint sensitivity analysis in nuclear reactor fuel behavior modeling. Nucl. Eng. Des. 66, 125–139.

Draper, N., Smith, H., 1998. Applied Regression Analysis. John Wiley & Sons.

Geelhood, K., Luscher, W., Beyer, C., 2011a. FRAPCON-3.4: A computer code for the calculation of steady-state thermal-mechanical behavior of oxide fuel rods for high burnup. Technical Report NUREG-CR-7022, Vol. 1. Pacific Northwest National Laboratory.

Geelhood, K., Luscher, W., Beyer, C., 2011b. FRAPCON-3.4: Integral assessment. Technical Report NUREG-CR-7022, vol. 2. Pacific Northwest National Laboratory.

Geelhood, K., Luscher, W., Beyer, C., Senor, D., Cunningham, M., Lanning, D., Adkins, H., 2009. Predictive bias and sensitivity in NRC fuel performance codes. Technical Report NUREG-CR-7001. Pacific Northwest National Laboratory.

Glaeser, H., 2008. GRS method for uncertainty and sensitivity evaluation of code results and applications. Sci. Technol. Nucl. Installations 2008, 798901.

Glen, G., Isaacs, K., 2012. Estimating sobol sensitivity indices using correlations. Environ. Model. Softw. 37, 157–166.

Homma, T., Saltelli, A., 1996. Importance measures in global sensitivity analysis of model output. Reliability Eng. Syst. Safety 52, 1–17.

Ikonen, T., 2012. Variance decomposition as a method of statistical uncertainty and sensitivity analysis of the fuel performance code FRAPCON-3.4. Technical Report VTT-R07723-12. VTT Technical Research Center of Finland.

Ionescu-Bujor, M., Cacuci, D., 2004. A comparative review of sensitivity and uncertainty analysis of large-scale systems – I: Deterministic methods. Nucl. Sci. Eng. 147, 189–203.

Jansen, M., 1999. Analysis on variance designs for model output. Comput. Phys. Commun. 117, 35–42.

Kvam, P.H., Vidakovic, B., 2007. Nonparametric Statistics with Applications to Science and Engineering. John Wiley & Sons.

Lilburne, L., Tarantola, S., 2009. Sensitivity analysis of models with spatially-distributed input. Int. J. Geogr. Inform. Sci. 23, 151–168.

Press, W., Teukolsky, S., Vetterling, W., Flannery, B., 2002. Numerical Recipes in C, 2nd edition. Cambridge University Press.

Rashid, J., Yagnik, S., Montgomery, R., 2011. Light water reactor fuel performance modeling and multi-dimensional simulation. J. Miner. Met. Mater. Soc. 63 (8), 81–88.

Sallaberry, C.J., Helton, J.C., 2006. An introduction to complete variance decomposition. In: IMAC-XXIV: Conference & Exposition on Structural Dynamics.

Saltelli, A., 2002. Making best use of model evaluations to compute sensitivity indices. Comput. Phys. Commun. 145, 280–297.

Saltelli, A., Annoni, P., 2010. How to avoid a perfunctory sensitivity analysis. Environ. Model. Softw. 25, 1508–1517.

Saltelli, A., Annoni, P., Azzini, I., Campolongo, F., Ratto, M., Tarantola, S., 2010. Variance based sensitivity analysis on model output. Design and estimator for the total sensitivity index. Comput. Phys. Commun. 181, 259–270.

Saltelli, A., Ratto, M., Andres, T., Campolongo, F., Cariboni, J., Gatelli, D., Saisana, M., Tarantola, S., 2008. Global Sensitivity Analysis. The Primer. John Wiley & Sons.

Sobol', I., 1967. Distribution of points in a cube and approximate evaluation of integrals. USSR Comput. Math. Math. Phys. 7, 86–112.

Sobol', I., 1993. Sensitivity analysis for non-linear mathematical models. Math. Model. Comput. Exp. 1, 407–414.

Syrjälahti, E., 2006. New sensitivity analysis tool for VTT's reactor dynamic codes. In: IYNC 2006, International Youth Nuclear Congress.

Wilderman, S., Was, G., 1984. Application of adjoint sensitivity analysis to nuclear reactor fuel rod performance. Nucl. Eng. Des. 80, 27–38.